Atmospheric
Chemistry
and Physics

Measurement report: An exploratory study of fluorescence and cloud condensation nuclei activity of urban aerosols in San Juan, Puerto Rico

Bighnaraj Sarangi[1], **Darrel Baumgardner**[2], **Benjamin Bolaños-Rosero**[3], and **Olga L. Mayol-Bracero**[1,a]

[1]Department of Environmental Sciences, University of Puerto Rico – Río Piedras Campus,
San Juan, Puerto Rico, USA
[2]Droplet Measurement Technologies, LLC, Longmont, Colorado, USA
[3]Department of Microbiology and Medical Zoology, School of Medicine, University of Puerto Rico –
Medical Sciences Campus, San Juan, Puerto Rico, USA
[a]now at: Environment and Climate Sciences Department, Brookhaven National Laboratory,
Upton, New York, USA

Correspondence: Bighnaraj Sarangi (bighnarajsarangi1986@gmail.com)

Abstract. Many atmospheric aerosols are cloud condensation nuclei (CCN), capable of activating as cloud droplets when the relative humidity exceeds 100 %. Some primary biological aerosol particles (PBAPs), such as plant spores, pollen, or bacteria, have been identified as such CCN. Urban environments are a source of these bioaerosols, some of which are naturally produced by the local flora or are transported from surrounding regions and others of which are a result of human activities. In the latter case, open sewage, uncovered garbage, mold or other products of such activities can be a source of PBAPs. There have been relatively few studies, especially in the tropics, where PBAPs and CCN have been simultaneously studied to establish a causal link between the two. The metropolis of San Juan, Puerto Rico, is one such urban area with a population of 2 448 000 people (as of 2020). To better understand the fluorescent characteristics and cloud-forming efficiency of aerosols in this region, measurements with a wideband integrated bioaerosol spectrometer (WIBS), a condensation nuclei (CN) counter and a CCN spectrometer were made at the University of Puerto Rico – Río Piedras Campus. Results show that the CCN / CN activation ratio and the fraction of fluorescing aerosol particles (FAPs) have repetitive daily trends when the FAP fraction is positively correlated with relative humidity and negatively correlated with wind speed, consistent with previous studies of fungi spores collected on substrates.

The results from this pilot study highlight the capabilities of ultraviolet-induced fluorescence (UV-IF) measurements for characterizing the properties of FAPs as they relate to the daily evolution of PBAPs. The use of multiple excitation and emission wavelengths, along with shape detection, allows the differentiation of different PBAP types. These measurements, evaluated with respect to previous, substrate-based analysis of the local fungal and pollen spores, have established a preliminary database of measurements that future, longer-term studies will build upon.

1 Introduction

The formation and evolution of clouds over the tropical island of Puerto Rico have been studied over the course of many years, primarily with respect to the sources of cloud condensation nuclei (CCN). Puerto Rico has been the site of these studies because of the fair weather, maritime flow and mostly clean atmosphere that leads to a mountaintop cloud that forms quite frequently throughout the year and can persist for several days (Allan et al., 2008; Gioda et al., 2013; Spiegel et al., 2014; Valle-Díaz, et al., 2016; Raga et al., 2016; Torres-Delgado, 2021). In addition to the clean, maritime sources, the cloud studies have also identified particles produced from urban areas, locally on the island of Puerto Rico and upwind from islands to the east, where vehicular and industrial emissions produce anthropogenic particles with organic carbon and sulfate compounds (Allan et al., 2008). Apart from this, clouds and rainwater in this region are influenced by natural aerosols that have undergone long-range transport, e.g., African dust, which is also potentially an important source of CCN, although the results are not conclusive as to how much cloud properties differ in the presence of these particles (Spiegel et al., 2014; Valle-Díaz, et al., 2016; Raga et al., 2016; Torres-Delgado, 2021).

Airborne primary biological aerosol particles (PBAPs) are an important type of aerosol in the tropics (Gabey et al., 2010, 2013; Stanley et al., 2011) that can encompass viruses (0.01–0.3 µm), pollen (5–100 µm), bacteria and bacteria agglomerates (0.1–10 µm), and fungal spores (1–30 µm) as well as mechanically formed particles, such as dead tissue and plant debris (Fennelly et al., 2017). Furthermore, there is evidence that PBAPs may influence the hydrological cycle and climate by initiating the ice nucleation process or acting as giant CCN (Möhler et al., 2007; Pope, 2010). Bioaerosols contribute a relatively small fraction (50 Tg yr^{-1}) of the total natural global emissions ($\sim$ 2900–13 000 Tg yr^{-1}) (Hoose et al., 2010; Stocker et al., 2013); however, their mass and number concentrations are site-specific and vary greatly depending upon the location and climatic conditions (Zhang et al., 2021, and references therein). In terrestrial ecosystems, bioaerosols constitute a major fraction, up to 30 %, of the total aerosol number concentration of coarse-mode particles, i.e., those > 1 µm (Fröhlich-Nowoisky et al., 2016). There is additional evidence that this number fraction is even larger in the urban air (Jaenicke, 2005). Upon emission from the biosphere, PBAPs undergo various physicochemical changes (e.g., coagulation, photooxidation and surface coating) and are removed through dry and wet deposition. These large PBAPs play a special role in precipitation development as giant CCN because they activate as larger droplets that more easily collide and coalesce to form raindrops. Hence, although small in number concentration, their size and capacity to contribute to early precipitation development make PBAPs potentially significant aerosols that impact the hydrological cycle.

Puerto Rico is characterized by a tropical climate, urban land cover and land use, moist soils, unique topography, and dense vegetation. These factors, associated with the easterly trade winds, influence the properties of atmospheric particles (Velázquez-Lozada et al., 2006). In addition, meteorology (i.e., humidity, temperature and winds) plays an important role, especially during the rainy season when fungal spores are predominantly released. The air quality of Puerto Rico suffers at times as a result of anthropogenic activities, African dust storms and volcanic eruptions on nearby islands. Emissions from the local pharmaceutical and power generation plants are responsible for releasing millions of pounds of air pollutants annually as well as a large number of organic compounds (e.g., *n*-alkanes, esters, phthalates, siloxanes and others), including plasticizer released into the atmosphere, which could pose a major health threat in this area (Torro-Heredia et al., 2020). The bioaerosol population on the island of Puerto Rico, in particular in the capital city of San Juan, has been studied extensively using the analysis of substrate samples (Quintero et al., 2010; Rivera-Mariani et al., 2011, 2020). The objective of the majority of these studies has been to evaluate the health effects of fungal and pollen spores on the local population (Quintero et al., 2010; Rivera-Mariani et al., 2011; Ortiz-Martínez et al., 2015; Rivera-Mariani et al., 2020). The studies by Quintero et al. (2010) are particularly relevant to the investigation reported here because they classified a wide variety of fungal and pollen spores that were the most responsible for respiratory ailments suffered by the residents of San Juan. In addition, they could link the relative number concentration of these spores to meteorological factors like relative humidity and wind speed. Given that these prior studies demonstrated that bioaerosols are a significant contributor to the aerosol population in Puerto Rico as well as the fact that other work has studied the role of marine aerosol and anthropogenic CCN in cloud formation over the island, a question arises regarding the apparent importance of bioaerosol as a source of CCN in this tropical region.

Prior to embarking on a longer-term project to evaluate PBAPs and CCN, under a wide range of conditions, a pilot study was designed and executed to investigate the properties of bioaerosols and CCN during September 2019. September was selected because the Quintero et al. (2010) results show that this time of the year is when peak concentrations of bioaerosol spores are found, and it is also a month of frequent cloud formation.

Considerable progress has been made in the development of technologies based on ultraviolet light-induced fluorescence (UV-LIF) (Ho, 1999; Huffman and Santarpia, 2017) for identifying PBAPs that fluoresce when excited at UV wavelengths. The wideband integrated bioaerosol spectrometer (WIBS) and the ultraviolet aerodynamic particle sizer (UV-APS) are examples of such instruments that measure the optical properties of individual particles over a moderately large size range (Savage et al., 2017). The WIBS and

the UV-APS have been used in studies including the ice nucleation activity of bioaerosol (Twohy et al., 2016), measurement of fungal spore concentrations (Gosselin et al., 2016), and investigation of long-range-transported bioaerosol in the tropics (Gabey et al., 2010; Whitehead et al., 2016) and at high altitudes (Gabey et al., 2013). The WIBS was developed by the University of Hertfordshire and commercialized by Droplet Measurement Technologies, LLC. In parallel with the WIBS measurements, the CCN and condensation nuclei (CN) number concentrations were also measured to investigate the links between fluorescing aerosol particles (FAPs), used here as proxies for bioaerosols, and cloud-forming particles and the total aerosol population, represented by the CCN and CN measurements, respectively.

The primary objectives of this exploratory, pilot study are to (1) measure the number concentrations of CN, CCN and FAPs; (2) identify correlations between CCN and FAPs; (3) analyze trends related to meteorological factors; and (4) compare the FAP measurements with those from previous studies that documented fungal and pollen spores using off-line analyses.

2 Measurement and analysis methodology

2.1 Measurement site and experimental setup

The CN, CCN and FAP measurements were made (Fig. 1a) at the Facundo Bueso (FB) building on the University of Puerto Rico, Río Piedras (UPR-RP) Campus (18°24′6.4″ N, 66°03′6.5″ W; 6 m a.m.s.l., above mean sea level). The spores were collected using a Hirst-type Burkard sampler (Burkard Scientific Ltd, Uxbridge, UK) located on the rooftop of the Medical Sciences Campus (MSC) of the University of Puerto Rico (18°23′48″ N, 66°4′30″ W; 60 m a.m.s.l.). The university is located in the capital city of San Juan (population of 2 448 000) which covers an area of 199 km^2. San Juan has a tropical climate with an annual rainfall of 107 ± 33 mm. The particles sampled at the measurement sites arrive from various sources, primarily from residential cooking, roadway traffic and vegetation.

2.2 Instrumentation

Sampling was performed for 8 consecutive days (16–23 September 2019). The measurement setup consisted of two diffusion dryers (TSI model 3062) connected in series, a cloud condensation nuclei counter (CCN-100, Droplet Measurement Technologies, LLC), condensation particle counter (CPC, TSI model 3772) and a wideband integrated bioaerosol spectrometer (WIBS-NEO, Droplet Measurement Technologies, LLC) (Fig. 1b). The samples were drawn from the exterior through the sidewall of the laboratory ($\sim$ 3 m a.g.l., above ground level) with conductive tubing (1/4 in. internal diameter and 1 m length). The aerosols were dried as they passed through two diffusion dryers

($< 10\%$ RH) containing silica gel before entering a manifold connected to the WIBS, CCN-100 and CPC, which sampled at flow rates of 0.3, 0.5 and 1 L min^{-1}, respectively. Particle losses due to sedimentation, diffusion and inertial separation along the sampling lines were calculated for each of the instruments (Kulkarni et al., 2011). The particle sampling efficiencies with respect to particle size are shown in the Supplement (Fig. S1). The sampling efficiency calculated for the particle size range from 0.1 to 3 μm is greater than 80%, decreasing to 60% at larger sizes. At this time, there have been no corrections applied for these losses. The WIBS derives an equivalent optical diameter (EOD) from the light scattered by individual particles that pass through a focused laser beam. The EOD is defined as the size of a particle scattering the equivalent intensity of light as a spherical particle with a known refractive index. Given that bioaerosols, dust and other types of environmental aerosols are not spherical, and their refractive index is unknown, the geometric size can be estimate to, at best, $\pm 20\%$; hence, relative size is more relevant than absolute size in our current analysis.

The CCN-100 is a continuous-flow, thermal-gradient, diffusion chamber that measures the concentration of aerosols activated as cloud droplets as a function of supersaturation (SS). Aerosol samples are drawn into a 50 cm tall column (inner diameter of 2.3 cm) whose inner walls are saturated with water. A series of heaters along the column are controlled to maintain a gradient from colder to warmer temperatures as the particles move down the column. As water vapor from the wetted column diffuses to the particles faster than the heat, a supersaturated condition is maintained that is determined by the temperature gradient and flow rate. Those aerosol particles that activate as cloud droplets at the constant SS in the chamber grow as the water molecules diffuse to the particle surfaces. An optical particle counter measures the number size distribution of the cloud droplets within the 0.75–10 μm size range as the activated droplets exit the chamber. The detailed operating principles and calibration procedures are described by Roberts and Nenes (2005). In our study, the supersaturation (SS) was maintained at 0.3%, which is a SS that is in the range of what would be encountered in convective clouds similar to those that form over the island of Puerto Rico (Duan et al., 2012; Uin et al., 2016).

The total concentration of environmental particles > 0.01 μm were measured with the CPC; during operation of this instrument, the aerosol sample is drawn continuously through a heated saturator in which butanol vapor diffuses into the aerosol stream. An external vacuum pump was used to draw the aerosol samples at 1 L min^{-1}. This CPC employs a single-particle-count mode to measure the particle number concentrations up to 10^7 L^{-1} at an accuracy $\pm 10\%$. The detailed design and working principle of the CPC are described by Stolzenburg and McMurry (1991).

The WIBS measures the fluorescent characteristics of aerosols using ultraviolet, light-induced fluorescence (UV-LIF) (Kaye et al., 2005; Stanley et al., 2011). This instrument
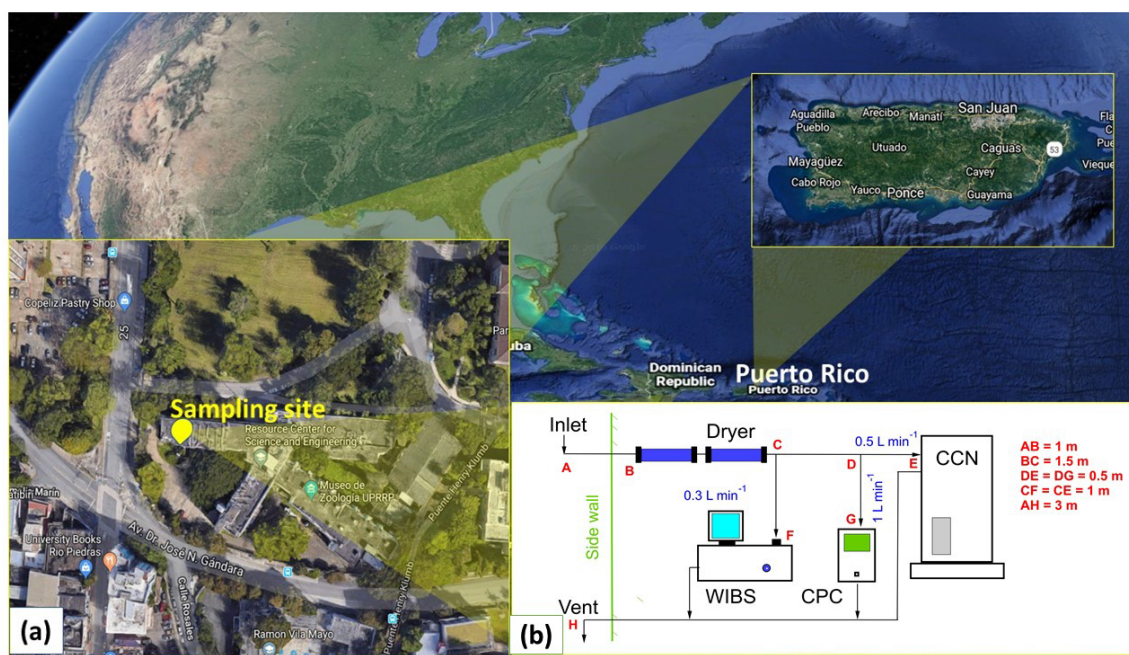
Figure 1. (a) The sampling location in the FB building of UPR-RP and **(b)** the experimental setup, comprising a cloud condensation nuclei (CCN) counter, a condensation particle counter (CPC) and a wideband integrated bioaerosol spectrometer (WIBS), are shown. This figure was generated using © Google Earth Pro 7.3.

provides detailed information on fluorescing bioaerosols on a single-particle basis. The detection principles of the WIBS are discussed elsewhere (Kaye et al., 2005) and briefly described here. Atmospheric particles are drawn into the WIBS via a laminar flow delivery system and pass through the beam of a continuous-wave diode laser (635 nm), which acts as a source for particle sizing and shape detection. The total flow is approximately $2.4 \, \mathrm{L \, min^{-1}}$ of which $2.1 \, \mathrm{L \, min^{-1}}$ is introduced in the form of sheath flow (i.e., filtered air) and $0.3 \, \mathrm{L \, min^{-1}}$ is sample flow to maintain the particle alignment with the 635 nm laser. The forward scattering of the light is detected by a quadrant photomultiplier tube (PMT) and is used to determine the asphericity factor (AF) of the particles, which roughly estimates the shape of the particles (Gabey et al., 2010). Experimental evidence shows that the AF is near 0 for a spherical particle, whereas it approaches 100 for a fiber or rod-like particle (Kaye et al., 2007; Gabey et al., 2010). The light scattered is used to activate, sequentially, two xenon lamps that are filtered to illuminate the particles with 280 and 370 nm light, respectively. The wavelengths were specifically selected to excite fluorescence in particles containing tryptophan (280 nm) and nicotinamide adenine dinucleotide with hydrogen (NADH, 370 nm). Examples of molecules containing tryptophan or NADH are proteins, vitamins, large polymers, molecules with conjugated double bonds and heterocyclic aromatic compounds, particularly when nitrogenous substituents are present. Tryptophan is an amino acid that has the highest ($\sim 90\%$) fluorescence in the native protein. Nicotinamide adenine dinucleotide phosphate (NADPH) is

one of the major contributors to the fluorescence signal when attached to the protein molecule and is produced widely in the metabolic cell. The fluorescence is recorded by the PMT detectors filtered at 310–400 and 420–650 nm. Hence, when a particle is excited at either of the incident wavelengths, there are four possible responses: (1) no fluorescence detected; (2) when excited at 280 nm, the particle fluoresces at a wavelength in the 310–400 nm waveband (FL1); (3) when excited at 280 nm, the particle fluoresces at a wavelength in the 420–650 nm waveband (FL2); or (4) when excited at 370 nm, the particle fluoresces at a wavelength in the 420–650 nm waveband (FL3). The fluorescence characteristics of an individual particle are determined in any of the three fluorescence channels when its fluorescence emission intensity exceeds a baseline threshold. The baseline threshold is determined using the approach by Perring et al. (2015) that incorporates the daily data sets to remove background artifacts. Particles that exhibit fluorescence lower than the baseline threshold were treated as nonfluorescent particles. A particle that fluoresces when excited by either of the xenon lamps may also produce emissions in both the 310–400 and 420–650 wavelength regions; hence, from the FL1, FL2 and FL3 signals, there are seven possible combinations that are designated fluorescence types A, B, C, AB, AC, BC and ABC (Perring et al., 2015). Types A, B and C refer to particles that fluoresce only in FL1, FL2 and FL3. The other four types are the respective combinations of the A, B and C.

It should be noted that the A and C types are highly sensitive to fluorescent bioaerosol particles, whereas the B

channel is cross-sensitive to nonbiological aerosols like certain organic compounds (Gabey, 2011). Based on the above description, the WIBS records the EOD, AF, fluorescent excitation–emission matrix and the total number concentration (N_{WIBS}), which includes nonfluorescing and total FAPs within the size range from 0.5 to 30 μm. Before deployment the WIBS was factory calibrated for the size, sphericity and fluorescence using reference fluorescent polystyrene latex spheres which are traceable to National Institute of Standards and Technology (NIST).

It is important to emphasize that, although the WIBS was designed to detect fluorescence from biological particles, it is unable to unequivocally differentiate what type of bioaerosol fluoresced (e.g., if the particle was bacteria, fungus or pollen). There are a number of studies, such as those by Hernandez et al. (2016), that have used the WIBS in laboratory studies to characterize a variety of species of bacteria, fungi and pollen. Such studies have shown that these three types of bioaerosols fall in general categories of size and fluorescence type. These categories will be discussed later in this paper in the context of comparing the FAP characteristics in San Juan to those reported in controlled laboratory experiments.

All measurements from the three instruments are averaged over 5 min intervals. In addition, the particle-by-particle (PbP) data from the WIBS are used to create size distributions as well as to derive fluorescence properties and interrelationships in greater detail.

2.3 Fungal spore data

The fungal spore data were obtained from the Department of Microbiology and Medical Zoology of the Medical Sciences Campus at the University of Puerto Rico. The enumeration of outdoor spores used the 12-traverse methodology proposed by the British Aerobiology Federation (Caulton and Lacey, 1995). Airborne spores were collected using a volumetric Hirst-type sampler, specifically a Burkard (Burkard Scientific Ltd, Uxbridge, UK). This equipment was located on the rooftop of the Medical Sciences Campus of the University of Puerto Rico, 30 m a.g.l. The Burkard 24 h trapping system worked continuously with an intake of 10 L min^{-1}. Spores were impacted on a microscopic slide coated with a thin layer of 2 % silicon grease as the trapping surface. The slides were changed daily and mounted on polyvinyl alcohol (PVA) mounting media for microscopic examination. Counting was done on each preparation along 12 traverse fields every 2 h for a total of 12 h on the longitudinal traverses. Spores were identified based on their morphological differences (Quintero et al., 2010). The identification was performed by means of a bright-field optical microscope Nikon Eclipse 80i microscope (Nikon Manufacturing), using a 1000× magnification.

2.4 Meteorological data

Hourly meteorological data, including temperature (°C), relative humidity (RH, %), wind speed (WS, m s^{-1}) and wind direction (°), were provided by the Department of Natural Science at the UPR-RP Campus.

The 24 h air mass back trajectories, ending at 100 m a.m.s.l., were obtained from the Hybrid Single-Particle Lagrangian Integrated Trajectory model (Global Data Assimilation System, 1° resolution, HYSPLIT) to identify the aerosol sources.

3 Results and discussion

3.1 Time series

Figure 2a shows the temporal trends in particle number concentrations of CN, CCN (at 0.3 % SS) and N_{WIBS} (0.5–30 μm) averaged in 10 min intervals. The average particle number concentration measured by the CPC was $(3 \pm 1) \times 10^6$ L^{-1}. This value is higher than the CN number concentrations reported previously at other, more remote locations on the island, such as at the northeastern coastal site of the Cabezas de San Juan Nature Reserve and at the Pico del Este (East Peak), in El Yunque National Forest, where the CN concentrations were $(9 \pm 5) \times 10^5$ and $(11.6 \pm 3) \times 10^5$ L^{-1}, respectively, both as reported by Allan et al. (2008). The differences in CN concentrations are primarily related to the geographical locations of the sites. The university measurement site is an urban location influenced by anthropogenic emissions, whereas Cabezas de San Juan is a remote coastal location where the atmosphere is relatively clean, influenced by marine aerosols or long-range-transported aerosols. The Pico del Este is a mountainous region that has a significant influence from aerosol from the nearby vegetation and from particles transported from the marine boundary layer. The CN concentrations show systematic, daily trends that reflect the emissions from motorized vehicle traffic and nearby residential heating and cooking. The mean CCN concentration of $(1.5 \pm 0.5) \times 10^5$ L^{-1} is about 20 times lower than the CN, suggesting that particles over the site are mostly nonhygroscopic or of low hygroscopicity, as would be expected of particles with anthropogenic origin (e.g., organic or black carbon).

The number concentrations of N_{WIBS} and FAPs were $(7.3 \pm 5) \times 10^4$ and $(5 \pm 3) \times 10^3$ L^{-1}, respectively, which are approximately 40 and 600 times lower than the CN concentrations. Given the differences in the lower size thresholds for the CPC and WIBS with respect to the smallest detectable particle (10 and 500 nm for the CPC and WIBS, respectively), this implies that about 98 % of the particles are smaller than 500 nm. The FAP concentrations showed a systematic, daily cycle in which nighttime particle concentrations were relatively higher than during the daytime. This trend is being driven primarily by the FAP type ABC, as illus-

trated in Fig. 2b where these concentrations are mostly much higher than the other six types. The type AB and AC concentrations have trends similar to type ABC, although their absolute magnitudes are much lower.

In the time series of number concentrations in Fig. 2, there is what appear to be periodicity in the CN, CCN and FAPs. This periodicity is seen more clearly in the concentrations averaged by the time of the day (over the whole measurement period), as shown in Fig. 3a and b. Figure 3a highlights the diel trend in CN concentration (black curve) that reaches an initial peak at 07:00 LT (local time) then a second peak four hours later at 11:00 LT. The CCN concentrations (blue curve) have morning peaks at 04:00 and 09:00 LT followed by a peak of much higher magnitude at 16:00 LT. The N_{WIBS} (magenta) first peaks at 07:00 LT, similar to the CN, followed by a second maximum 1 h after the CCN peak. The FAP concentrations remain elevated between midnight and 06:00 LT, after which they decrease by about 30 % and remain fairly constant the remainder of the day. The FAPs are dominated by type ABC particles in the morning hours, during which time their concentrations are 4 times larger than all other types, as shown in Fig. 3b.

All other FAP types remain approximately constant throughout the day except for type AC, which follows the trend of type ABC, although at significantly lower concentrations.

3.2 Temporal trends in the particle size distribution

Figure 4 shows the size distributions of the total (Fig. 4a) and FAP (Fig. 4b) number concentrations averaged in 10 min intervals. The color scale is the log of the concentration. The white curves are the average median volume diameters. The total number size distributions show an irregular trend of increasing concentrations over all sizes, usually occurring around midday on all days except on the day of the year (DOY) 264 when the size distributions remain approximately the same throughout the day. In contrast, the FAP size distributions have a more regular daily pattern whereby the concentrations increase over all sizes to a maximum between midnight and 06:00 LT. This reflects a similar trend to that illustrated in the daily FAP concentrations in Fig. 3a.

The daily trends in the size distributions of the seven different types of fluorescent particles are shown in the Supplement (Fig. S2). We observe that the ABC- and AB-type particles are dominant at the site and have a unique and systematic diel cycle. Reflecting the behavior of the total concentrations in Fig. 3b, the average EODs of ABC- and AB-type particles increase at night, and the particle size grows to $> 4\,\mu m$ by midnight. Fluorescent type A does not show any specific temporal trend, whereas types B and C have periods when the concentrations increase over all sizes but do not follow the trends in the ABC- and AB-type particles. The type BC and AC particle concentrations are much lower than the other types.

The increases in the modal diameter from daytime to nighttime, as seen in the Supplement (Fig. S2), particularly for types AB, AC and ABC, were further investigated by comparing the size distributions averaged at night and during the daytime. We have plotted the particle size distributions for these three FAP types (Fig. 5), averaging from 12:00 to 18:00 LT (red shading) and from 24:00 to 06:00 LT (blue shading) over the whole measurement period (DOY 259–266). These two periods represent the time intervals when the number concentrations and average sizes exhibit the largest differences. All three FAP types show a shift towards larger sizes from daytime to nighttime; however, type ABC particles have the most distinctive shifts (Fig. 5c), which are indicative of a general increase in concentration over all sizes but with a very clear, larger increase at EODs larger than $2\,\mu m$.

3.3 Asphericity

The asphericity, derived from the quad detector of the WIBS, is a relative indicator of the shape of each particle, as shown in the Supplement (Fig. S3) for FAP types (AB, AC and ABC) and for all particles, including nonfluorescent particles (non-FAPs). The color scale shows the average asphericity at each size interval over the duration of the project. Among the fluorescent types, the asphericity of ABC particles shows the most dominant mode between 2 and $4\,\mu m$ during nighttime, especially at midnight. The asphericity size distributions of all particles show a broader mode of enhanced asphericity between 2 and $4\,\mu m$ that varies somewhat but not in a noticeable diel pattern. Note that particles with asphericity values < 20 are generally considered quasi-spherical; thus, the values that are shown here indicate slight changes in shape, on average, of type ABC particles, as well as all particles, but the overall population of particles can be considered quasi-spherical.

The asphericity of non-FAPs was always observed to be higher than that of FAPs (Fig. S3d in the Supplement). The higher asphericity values of non-FAPs can be seen between a size of 3 and $6\,\mu m$ every day and dominate on DOY 261 and 262.

3.4 Air mass back trajectories

The air masses that arrived at the measurement site on DOY 259 and 264 had been over the Atlantic Ocean, northeast of the island, 24 h earlier, whereas air masses arrived from the southeast on DOY 260–63 and 266 and from the south-southeast on DOY 265. Figure S4a shows that the air masses on all days had been < 50 m a.g.l. for the entire 24 h period before arriving at the measurement site. The one exception was on DOY 259 when an air mass had stayed above 200 m a.g.l. from 12 to 24 h before arriving at the measurement site and then began descending as it approached the island. This same air mass was associated with rain forma-
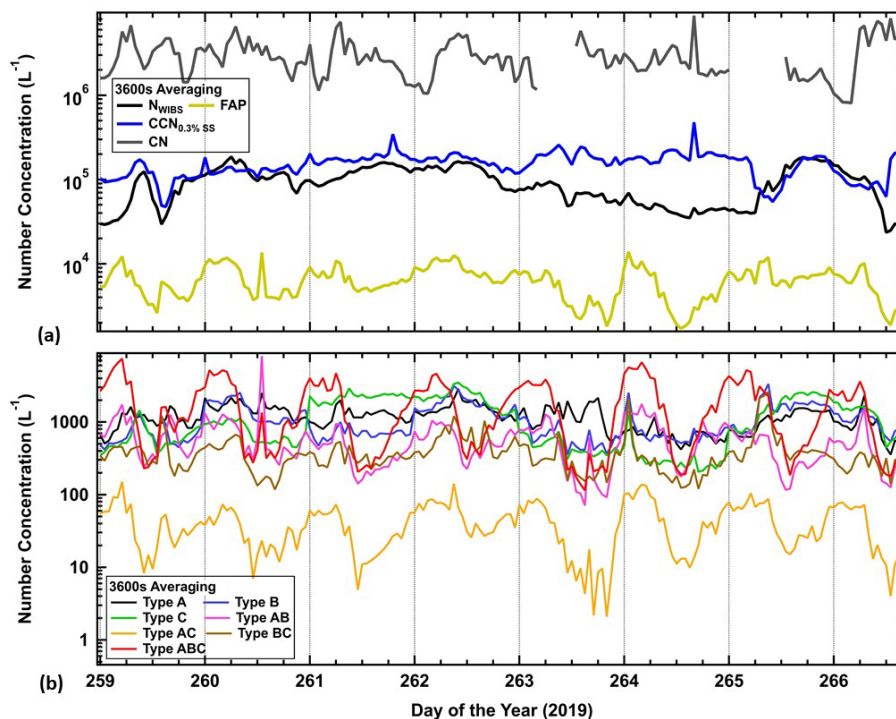
Figure 2. Time series of the number concentrations of **(a)** CN, CCN, N_{WIBS} and FAPs as well as of **(b)** FAP types A, B, C, AB, AC, BC and ABC. The gaps in time in the CN concentrations were when the CPC was offline.
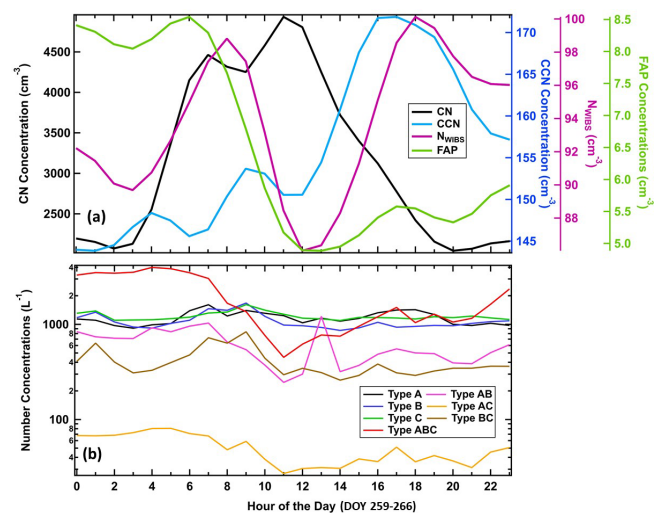

Figure 3. (a) Hourly concentrations of CN (black curve) and CCN at 0.3 % supersaturation (solid blue curve), N_{WIBS} (magenta) and FAP (green) concentrations. **(b)** Hourly concentrations of the seven types of FAPs.

tion close to the measurement site (Fig. S4b in the Supplement). The air mass on DOY 264 came across the islands to the southeast of Puerto Rico (e.g., Culebra and the British Virgin Islands), possibly mixing marine aerosols with polluted emissions before arriving at the measurement

site. Likewise, the air mass trajectory on DOY 260 and 262 crossed over Vieques and the Virgin Islands of the United States at a low altitude, also mixing with anthropogenic emissions. The increment in total particle number concentrations on DOY 260–262 and DOY 266, shown in Fig. 4a, is possibly attributed to these air mass that passed over the populated islands to the southeast of Puerto Rico and may also be the reason why we observed higher asphericity values for non-FAPs on DOY 261 and 262. The remainder of the air masses were presumably not impacted by anthropogenic emissions until they arrived over the landmass of Puerto Rico.

3.5 Meteorological data

Figure S5 shows the temperature and relative humidity (RH) (Fig. S5a) as well as the wind speed, wind direction and precipitation (Fig. S5b). The average wind speed, temperature and RH values for the period of measurement were $2.8 \pm 2.4\,\mathrm{m\,s^{-1}}$, $29 \pm 2\,°\mathrm{C}$ and $77 \pm 11\,\%$, respectively. DOY 259 and 265 received significant rainfall of 34 and 47 mm, respectively. Note that these 2 days are associated with those air masses whose analysis indicated precipitation along their back trajectories. The wind speed and direction, temperature, and RH show a systematic daily cycle: the wind speed and temperature peaked during the midday hours ($2.8 \pm 0.7\,\mathrm{m\,s^{-1}}$ and $33 \pm 1\,°\mathrm{C}$, respectively), and the RH peaked around midnight ($91 \pm 3\,\%$). At the measurement site, the winds were from 135 to 250° during the night and
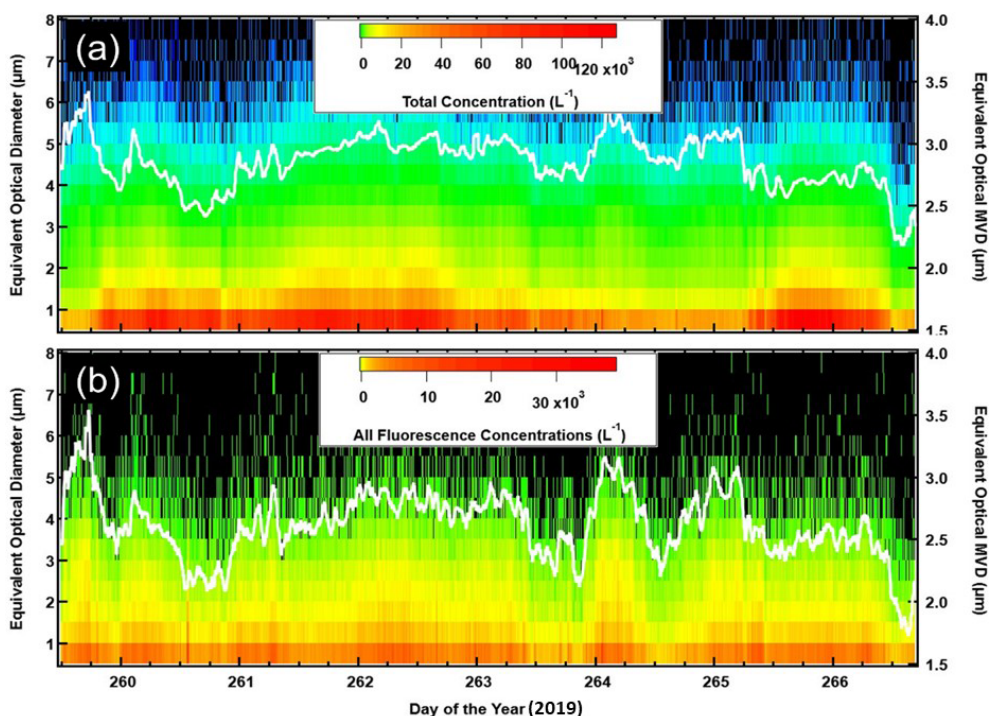
Figure 4. Time series of **(a)** total and **(b)** fluorescent particle size distributions measured by WIBS for the period from 16 to 23 September (DOY 259–266) 2019. The white curves are the average median volume diameters (MVDs).
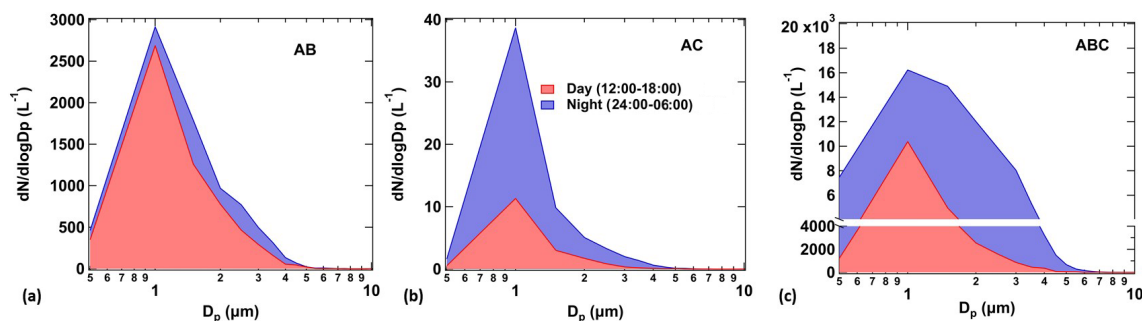

Figure 5. The size distributions of types **(a)** AB, **(b)** AC and **(c)** ABC were averaged from 12:00 to 18:00 LT (red shading) and from 24:00 to 06:00 LT (blue shading) for the 8 d of the project.

shifted to coming from 93 to 134° during the daytime. On DOY 262 and 265 as well as the afternoon of DOY 259, the winds were comparatively low at night ($0.24 \pm 0.2 \, \mathrm{m \, s^{-1}}$) compared with those during the day ($2.8 \pm 0.6 \, \mathrm{m \, s^{-1}}$), suggesting generally calm wind conditions that are normal at this time of year in the absence of the influence of tropical storms.

To further highlight the relationships between the meteorological conditions and FAPs, we computed the hourly averages of the RH, wind speed and FAP concentrations during each 24 h period over 8 d (Fig. 6a). The RH and FAP concentrations reached their maxima between the hours of midnight and 06:00 LT, whereas the wind speed was at a minimum during those hours.

The relationship between RH and the FAP fraction is highlighted in Fig. 6b and c: there appears to be an RH threshold of approximately 80 % below which the FAP fraction remains lower than 0.1; when the RH exceeds this value, the FAP fraction increases rapidly to its maximum value of 0.3. The color coding indicates the median volume diameter (Fig. 6b) and number concentration (Fig. 6c). In both cases, the size and concentration increase when the RH exceeds 80 %. The increase in the FAP volume-weighted equivalent optical diameter (D_{mvd}) and the number concentrations depends on the hygroscopicity of the particles. Among the different FAPs measured at the site, the ABC, AB and AC types were observed to have systematic diel patterns and were believed to be more hygroscopic than the other types. There-

fore, the D_{mvd} and FAP number concentrations increased when RH reached 80 % and above.

3.6 Fungal spore data

The time series of the Hirst sampler fungal spores are shown in Fig. 7. Similar to the FAP number concentrations and fractions, the spore concentrations have a diel trend with average concentrations of $48 \pm 42 \, \text{L}^{-1}$ and a maximum of $112 \pm 44 \, \text{L}^{-1}$ around midnight. We calculated positive correlations of 0.7, 0.47 and 0.54 between the total spore concentration and concentrations of FAP types ABC, AB and AC, respectively. Previous studies for this region reported that the most common fungal genera detected were the basidiospores and ascospores (Quintero et al., 2010; Rivera-Mariani et al., 2011). Figure 7b illustrates how these fungal spore types were speciated. The broad categories are hyphae or filamentous spores, macroconidia $> 10 \, \mu\text{m}$, microconidia from 3 to $10 \, \mu\text{m}$, microconidia $< 3 \, \mu\text{m}$ and unidentified spores. We observed that the microconidia from 3 to $10 \, \mu\text{m}$ contributed the highest fraction (81 %) to the total fungal species followed by microconidia $< 3 \, \mu\text{m}$ (3.86 %) and macroconidia $> 10 \, \mu\text{m}$ (1.8 %). The basidiospores contributed the highest fraction (49.4 %) to the total fungal spores, followed by ascospores (19 %), Diatrypaceae (8.6 %), and *Penicillium* and *Aspergillus* (3.86 %). The mean concentrations of dominant species such as basidiospores, ascospores, Diatrypaceae, and *Penicillium* and *Aspergillus* were 24 ± 20, 9.3 ± 4, 4 ± 3 and $2 \pm 1 \, \text{L}^{-1}$, respectively. The ascospores as well as *Penicillium* and *Aspergillus* had more elevated concentrations during the night, whereas Diatrypaceae concentrations were generally higher during the daylight hours.

These species were the most common airborne spores in San Juan throughout the year and predominated during September (the rainy month); hence, the FAP types ABC and AB, measured by the WIBS, were likely the basidiospores and ascospores (Fig. 7b). Previous studies (Quintero et al., 2010; Rivera-Mariani et al., 2020) have reported that the most common fungal genera detected were the basidiospores and ascospores, which was confirmed in this study. The sizes of the basidiospores and ascospores $(10–20 \, \mu\text{m})$ are usually larger than those of *Aspergillus*, *Penicillium* and *Cladosporium* spores. Furthermore, we observed a systematic diel pattern in the number concentrations of these fungal spores that is strongly correlated with the diel pattern of ABC-type FAPs. The other genera most frequently detected were *Penicillium* and *Aspergillus*, *Cladosporium*, and *Ganoderma*, observed at low concentrations, as reported by Quintero et al. (2010). These species possibly corresponded to FAP type AC which was periodic but at relatively low concentrations. These fungal spores that occurred between midnight and the early morning period, suggest an active release mechanism induced by the high humidity during early morning hours under calm wind conditions, in accordance with the findings of Quintero et al. (2010).

4 Discussion

The preliminary results from this pilot study highlight the following: (1) the CN, CCN and FAP concentrations have daily patterns during which each reaches a maximum at a different hour of the day; (2) the periodic FAP concentration is predominantly of type ABC and reaches a daily maximum around midnight, during time which the asphericity of this type also increases; (3) the RH also reaches a maximum each day around midnight; (4) the wind speeds reach a minimum around midnight; and (5) an independent analysis of bioaerosols using fluorescence microscopy to identify spore types revealed a periodicity of spore concentrations that was highly correlated with the RH and FAP type ABC concentrations.

Referring back to Fig. 3a, the CN, CCN, N_{WIBS} and FAP concentrations all exhibit a diel periodicity but with differing, uncorrelated trends. The CN population encompasses all environmental particles larger than about 10 nm and is dominated by anthropogenic aerosols. Given that the WIBS measures the concentration of particles larger than $0.5 \, \mu\text{m}$ and that the total concentration has an average peak maximum of $100 \, \text{cm}^{-3}$, compared with a maximum CN concentration of $5000 \, \text{cm}^{-3}$, this implies that 98 % of the particles have sizes smaller than $0.5 \, \mu\text{m}$. A comparison of the maximum CCN and N_{WIBS} concentrations ($170 \, \text{cm}^{-3}$ versus $100 \, \text{cm}^{-3}$) leads us to conclude that most of the CCN are likely greater than $0.5 \, \mu\text{m}$ in size. Likewise, as the maximum CCN concentrations are only about 2 % of the CN values, this suggests that most of the CN have low hygroscopicity, which is a characteristic of fresh combustion particles.

The timing of the maxima in the CN concentrations suggest that the trends are a result of two traffic patterns: (1) the general city traffic related to workers commuting to jobs that are not on the university campus and (2) vehicular traffic related to university workers whose starting hours are later than the city workers. As shown in Fig. 1a, the sampling site is located near the intersection of two major avenues that carry both types of traffic.

The comparison between the times of the two N_{WIBS} maxima and the CN and CCN peaks suggests that the $> 0.5 \, \mu\text{m}$ particles measured with the WIBS in the morning are a different mixture of compositions than the particles in the afternoon. The morning N_{WIBS} peak lags the first CN peak by 1 h, which is likely the result of the primary emissions producing particles that grow into the size range measured by the WIBS; however, with the sunrise at around 06:00 LT, temperatures begin increasing, and the material in the more volatile particles begins to evaporate until the particle sizes decrease below the threshold of the WIBS. Some dilution will also be occurring as the boundary layer deepens with increasing temperatures, but this is a secondary effect, as we do not see the CN concentrations decrease with the decrease in N_{WIBS}. As the CCN concentrations remain low during this period, this implies that either the particles did not grow large enough
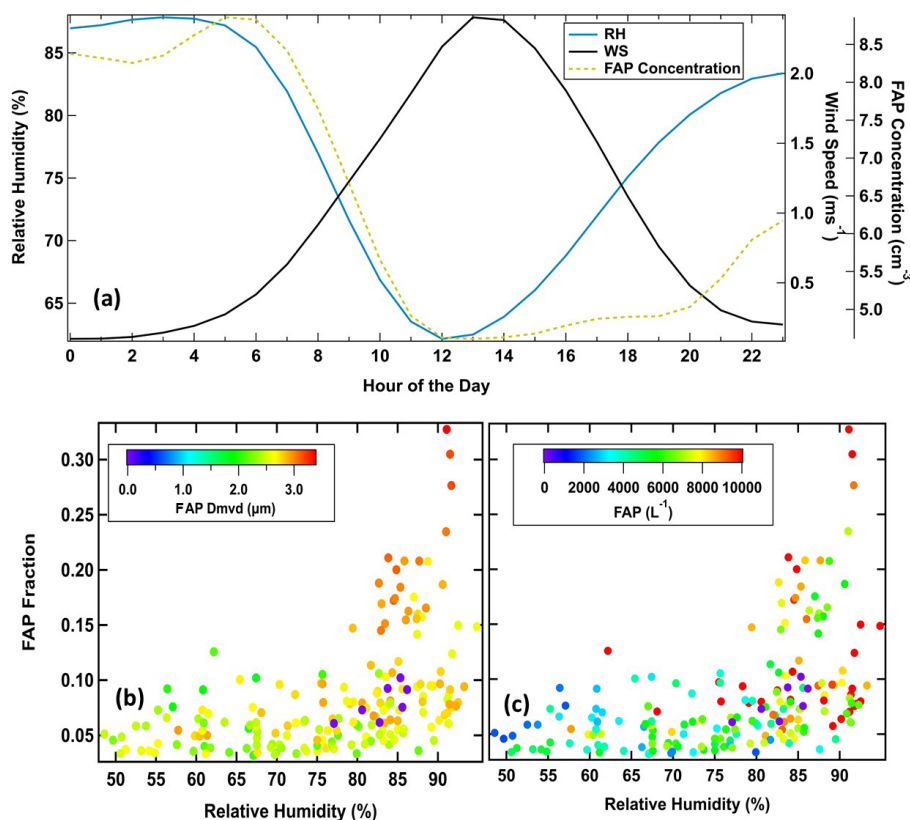
Figure 6. (a) Hourly averages of relative humidity (blue curve), wind speed (black curve) and FAP concentration (green dotted curve). **(b)** The link between the fluorescent fraction and relative humidity (FAP volume-weighted equivalent optical diameter. D_{mvd}, on the color scale). **(c)** The fluorescent fraction and relative humidity (FAP concentration on the color scale). The data in all figures are averaged over DOY 259–266.

to be good CCN or their composition is not conducive for forming CCN. In the early afternoon, we observe that the CCN concentrations increase until they reach their late afternoon peak. The N_{WIBS} follows a similar trend but lags with respect to the CCN by a couple of hours. This afternoon trend in CCN has been identified in other large, polluted urban areas as the result of photochemical reactions producing hygroscopic, secondary organic aerosols (SOAs) from photochemical reactions (Baumgardner et al., 2004). The N_{WIBS} is offset by a couple of hours due to the time needed for the SOA particles to grow by condensation and aggregation. Finally, the FAP concentrations only begin increasing late in the evening after the CCN reach a maximum and the FAP concentrations are less than 10 % of the CCN. This suggests that if FAPs are good CCN, they do not contribute significantly to the overall CCN population. It is important to note that contributions to the overall CCN population depend on size, chemical composition and the number concentrations of particles.

Quintero et al. (2010) concluded that the release of the fungal spores, those that they measured and speciated at multiple locations, was triggered by high RH. Pollen spores, on the other hand, could not be linked conclusively to any me-

teorological factor. Based on a comparison of the species of spores found at the University of Puerto Rico, compared with those measured in the El Yunque rain forest, Lewis et al. (2019) concluded that the rain forest was the likely source of the majority of the spores identified in the city of San Juan and, hence, at the university. Two of the air sampling sites, Pico Del Este (PDE) and Cabezas de San Juan (CSJ), are very similar and very low in fungal spores (less than 5000 spores m^{-3}). At another sampling site in El Verde (located to the west within El Yunque National Forest), the concentrations increase to 72 000 spores m^{-3} and are found to have a decreasing gradient of fungal spores towards the metro area. For the rest of Puerto Rico, the Central Mountain Range is the other major source of fungal spores. Hence, given these previous results, in comparison with the correlations that we have observed in the current study (Figs. 6, 7), type ABC fluorescing particles are most clearly linked to basidiospores and ascospores – the two species that made up the largest fraction of fungi measured with the fluorescence microscopy. The hourly averages in Fig. 3b also showed that type ABC only was predominant during the same period as the basidiospores and ascospores, whereas the other FAP types showed no obvious daily trends. This is mirrored by
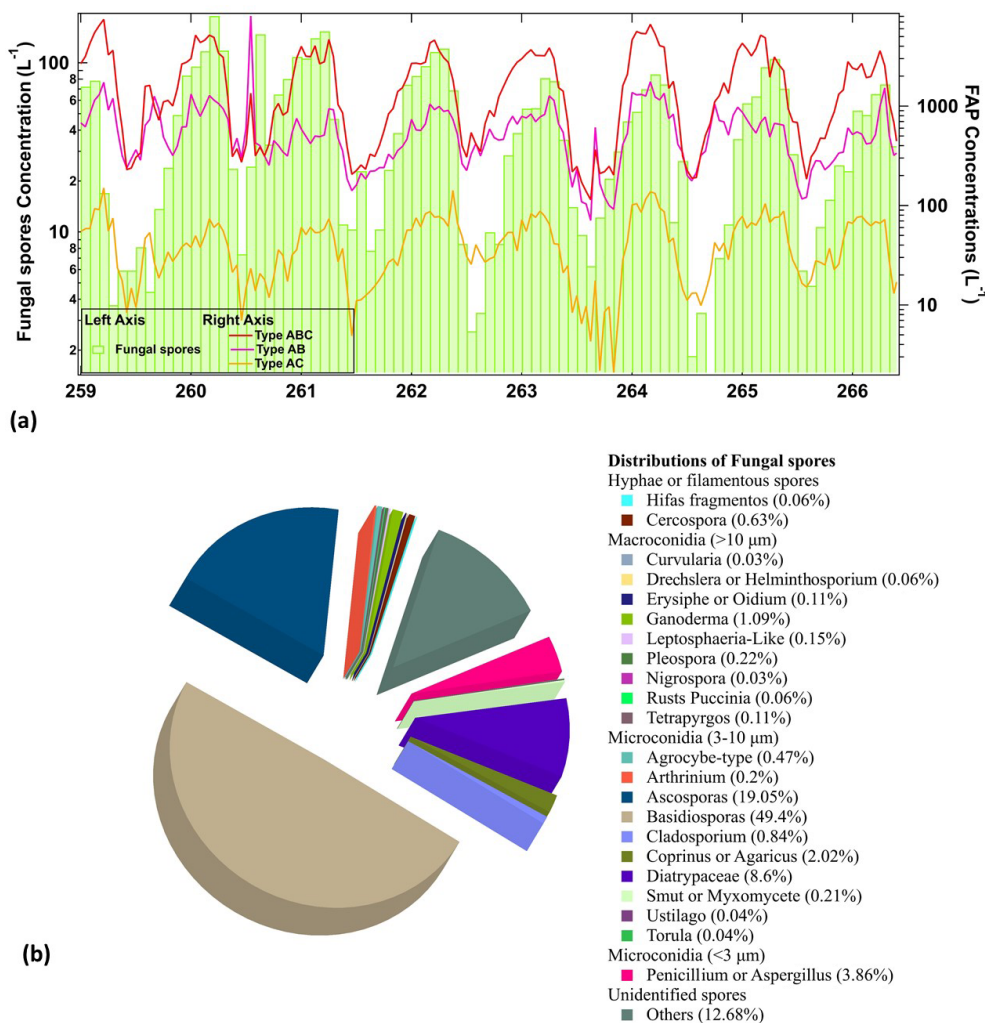
(a)

(b)

Figure 7. (a) Time series of the particle number concentrations of fungal spores (left axis), measured at the Department of Microbiology and Medical Zoology of Medical Sciences Campus at University of Puerto Rico, and the FAP types ABC, AB and AC (right axis) detected by WIBS. **(b)** Speciation of the outdoor fungal spores.

the spore types shown in Fig. 7 that change in relative mixture during the day.

The WIBS characterizes the fluorescent aerosol particles using two-wavelength excitations and two-wavelength emissions. The sensitivity of types A and B to the intensity of the emissions in the 310–400 and 420–650 nm wavelength bands, when excited at 280 nm, in comparison with the intensity of emissions at 420–650 nm when excited at 370 nm has been exploited in the study by Ziemba et al. (2016) to identify differences in bioaerosol types as they relate to differences in FAP sources. In their study, the abovementioned authors were able to show a clear grouping of FAPs linked to source regions by plotting the ratio of type A to type B (emission sensitive) versus the ratios of type C to type B (excitation sensitive). We have followed a similar scheme; however, whereas the study of Ziemba et al. (2016) used a WIBS on an airborne platform flying over various land use

types, we compute these ratios as a function of time rather than location because our site was fixed. Figure 8 illustrates the periodicity of the type C / B ratio, which increases during those time periods in which the type ABC concentrations were also increasing. Just as the FAP sizes were seen to increase during these periods (Fig. 5), which was indicative of a change in FAP type, the shift in the type C / B ratio reflects the differences in the fungal spore types.

Hence, the fact that the changes in size distribution, asphericity, type C / B ratios and speciated spore concentrations all occur during the same time of day provides independent verification that a different type of PBAP is being produced during periods of high RH than during other periods of the day.

The strong correlation between spore release and RH that has been highlighted in this study has been previously reported by studies such as Oliveira et al. (2005), Chi and
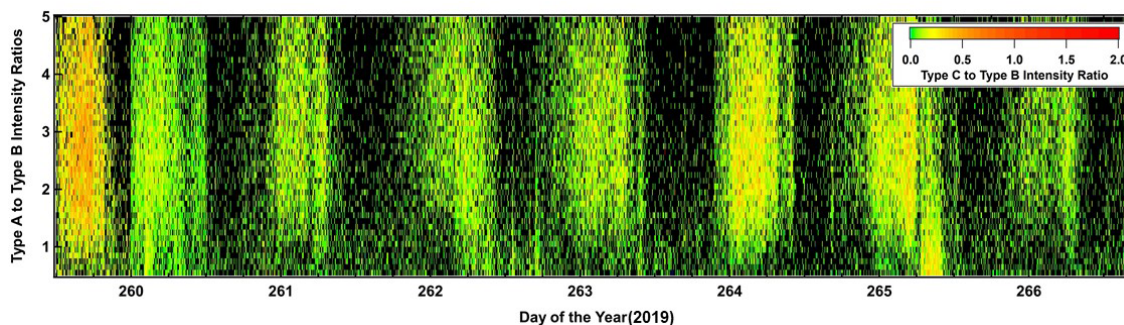
Figure 8. Temporal distribution of the emission wavelength dependence (type A to type B) versus excitation wavelength dependence (type C to type B).

Li (2007), Gabey et al. (2013), Calvo et al. (2018), Toprak and Schnaiter (2013), and Healy et al. (2014). However, none of these studies were from tropical regions nor did they include the asphericity and FAP type ratio approach to quantify their results.

Some laboratory studies have been conducted to measure the fluorescence characteristics of a small variety of bacteria, fungi and pollen; for example, Hernandez et al. (2016) determined that bacteria, fungi and pollen could be generally grouped according to their size and FAP type. In their study, very few fungal spores were of the FAP type ABC, in contrast to those found in the current study. Instead, the majority of their fungi were types A and AB, whereas the majority of type ABC spores were pollen, not fungi. On the other hand, the Hernandez et al. (2016) study did not test any of the major fungal species that were measured in the natural environment of Puerto Rico (i.e., basidiospores and ascospores). Hence, future laboratory studies that use the WIBS to measure fungal spores native to Puerto Rico should be a high priority.

5   Summary and conclusions

A pilot study was conducted to evaluate the fluorescence and cloud condensation nuclei (CCN) properties of urban aerosols in San Juan, Puerto Rico. This is the first time, to our knowledge, that such measurements have been made in this tropical city. Previous CCN measurements have been made on this island at coastal and rainforest sites, but no research has been pursued to see if bioaerosols are directly linked to CCN. There have been a number of laboratory studies conducted by other researchers that evaluated the CCN activity of various bacteria, fungi and pollen. Although some types of bioaerosols were found to be potential CCN, many others were not. Hence, the importance of bioaerosols as cloud-forming particles remains an open question. The very large concentrations of fungal spores produced by flora in Puerto Rico, as reported by Quintero et al. (2010), along with the results from our pilot study provided the initial motivation

for the work reported here to assess if bioaerosols might contribute to the frequent cloud formation over the island.

The measurements were made from the Facundo Bueso building at the University of Puerto Rico, Río Piedras Campus – an urban location that experiences emissions from anthropogenic activity and the production of fungal spores from a wide variety of flora within the university campus as well as from the nearby tropical forest – from 16 to 23 September 2019.

In the pilot experiment, the CCN and FAP concentrations were measured with a commercial CCN spectrometer and wideband integrated bioaerosol spectrometer (WIBS), respectively. It is important to note that bioaerosols are not the only type of aerosol particle that will display autofluorescence when excited at the wavelengths used in the WIBS, although care was taken to minimize interference from non-biological particles. Therefore, the results reported in the current study are the properties of fluorescing aerosol particles (FAPs) without specifically labeling them as biological. In addition to measurements of CCN and FAPs, the total concentration of condensation nuclei (CN) was documented with a condensation particle counter.

The mean number concentration measured by the CCN counter at 0.3 % SS was $(1.5 \pm 0.5) \times 10^5 \, \text{L}^{-1}$, which was about a factor 20 lower than the average CN concentration $(3 \pm 1) \times 10^6 \, \text{L}^{-1}$. The mean FAP concentration was $(5 \pm 3) \times 10^3 \, \text{L}^{-1}$, which was a small fraction ($\sim 7\%$) of the total aerosol particle number concentration (N_{WIBS}) measured by the WIBS, whose lower size threshold is 0.5 μm.

The CN, CCN, N_{WIBS} and FAP concentrations all have daily trends, but their maxima occur at different times of the day. The CN peaks at 06:00 and 11:00 LT due to business traffic and university traffic, which have different respective rush hours. The CCN reaches its maximum value at 16:00 LT as photochemical processes produce secondary organic aerosols (SOAs) that are likely hygroscopic in composition. The N_{WIBS} is bimodal, with a morning peak at 08:00 LT, reflecting rush hour emissions whose particles grow into the size range of the WIBS, and a second max-

imum at 18:00 LT, as the SOAs grow to measurable sizes. The diel trends in the FAP concentrations are not correlated with the CN, CCN nor N_{WIBS}, as they remain fairly constant throughout the daylight hours but then rapidly increase to their maximum value that extends from midnight until 06:00 LT.

The FAPs are classified according to the wavelengths at which they were excited and at which they emitted fluorescence. These types have been categorized as A, B, C, AB, AC, BC and ABC. In the current study, types A, B, C and ABC all had average concentrations of about $1000 \, \mathrm{L}^{-1}$ during the daylight hours, whereas the other three types were much lower in concentration; however, only type ABC showed a rapid increase in concentration, to almost $5000 \, \mathrm{L}^{-1}$, between midnight and 06:00 LT.

Independent measurements using fluorescent microscopy of spores captured on substrates were made during the same time period. Although more than 20 species of spores were identified with this technique, the fungi basidiospores and ascospores were not only the most predominant, but they were also the spores that followed an almost identical daily trend to the FAP type ABC (i.e., remaining nearly constant in concentration during the daylight hours and then increasing in the evening to a maximum between midnight and 06:00 LT).

The other environmental parameters that were also significantly correlated with the temporal trends in fungal spores and FAPs were the relative humidity (RH) and the wind speed. As the RH began to increase in the late afternoon, the spore counts and FAP concentrations also increased. A comparison of the RH with FAP concentrations indicates that the FAP concentrations begin increasing above an RH threshold of about 80 %. Spores are released by a number of species of fungi when the RH increases, as has been well documented in other studies (Quintero et al., 2010). Hence, the relationship between RH, basidiospores and ascospores, and ABC-type FAPs has been clearly established.

Three additional properties of FAPs were extracted from the WIBS measurements that provided indirect but complementary information showing how type ABC particles are related to basidiospores and ascospores: (1) the size distribution, (2) the asphericity, and (3) the excitation and emission sensitivity parameters. Firstly, the type ABC particles during the high-RH periods had much higher concentrations of particles larger than $2 \, \mu\mathrm{m}$ when compared with the size distributions of these same particles during the daylight hours. Secondly, the asphericity increased during periods with high concentrations of type ABC FAPs. Thirdly, the excitation and emission sensitivity parameters increased during this same period. While not quantitative, these three parameters confirmed that the particles whose concentrations were increasing during the abovementioned period had different properties than during other periods of the day.

As the trends in the CCN concentration were not directly correlated with FAPs, we cannot conclude that bioaerosols are a potential source of cloud-forming particles. In addition,

the FAP concentrations were less than 10 % of the CCN concentrations; thus, even if some FAPs are potential CCN, the clouds that develop over the island are more likely formed from other aerosol types than locally produced fungal spores.

The results from this pilot study have provided strong motivation for longer-term measurements that will expand the database of aerosol particle properties in this tropical, urban area. The detailed information on fungal spores in this region, in comparison with the multiparameter data available from the WIBS, will improve our ability to interpret these measurements of FAPs and apply this knowledge to data sets acquired in other parts of the world.

Author contributions. BS designed the study in consultation with OLMB and performed the measurements. BBR provided the measurements of fungal spore and pollen concentrations. DB and BS performed the analysis, interpreted the results, and wrote the paper with contributions from OLMB and BBR.

Competing interests. The contact author has declared that none of the authors has any competing interests.

Disclaimer. Publisher's note: Copernicus Publications remains neutral with regard to jurisdictional claims in published maps and institutional affiliations.

Review statement. This paper was edited by Ottmar Möhler and reviewed by two anonymous referees.

References

Allan, J. D., Baumgardner, D., Raga, G. B., Mayol-Bracero, O. L., Morales-García, F., García-García, F., Montero-Martínez, G., Borrmann, S., Schneider, J., Mertes, S., Walter, S., Gysel, M., Dusek, U., Frank, G. P., and Krämer, M.: Clouds and aerosols in Puerto Rico – A new evaluation, Atmos. Chem. Phys., 8, 1293–1309, https://doi.org/10.5194/acp-8-1293-2008, 2008.

Baumgardner, D., Raga, G. B., and Muhlia, A.: Evidence for the formation of CCN by photochemical processes in Mexico City, Atmos. Environ., 38, 357–367, https://doi.org/10.1016/j.atmosenv.2003.10.008, 2004.

Calvo, A. I., Baumgardner, D., Castro, A., Fernández-González, D., Vega-Maray, A. M., Valencia-Barrera, R. M., Oduber, F., Blanco-Alegre, C., and Fraile, R.: Daily behavior of urban Fluorescing Aerosol Particles in northwest Spain, Atmos. Environ., 184, 267–277, https://doi.org/10.1016/j.atmosenv.2018.04.027, 2018.

Caulton, E. and Lacey, M.: Airborne Pollens and Spores. A Guide to Trapping and Counting, 1st Edn., Harpenden, British Aerobiology Federation, ISBN 0952561700, 1995.

Chi, M. C. and Li, C. S.: Fluorochrome in monitoring atmospheric bioaerosols and correlations with meteorological factors and air pollutants, Aerosol Sci. Technol., 41, 672–678, https://doi.org/10.1080/02786820701383181, 2007.

Duan, J., Chen, Y., and Guo, X.: Characteristics of aerosol activation efficiency and aerosol and CCN vertical distributions in North China, Acta Meteorol. Sin., 26, 579–596, https://doi.org/10.1007/s13351-012-0504-6, 2012.

Fennelly, M. J., Sewell, G., Prentice, M. B., O'Connor, D. J., and Sodeau, J. R.: The Use of Real-Time Fluorescence Instrumentation to Monitor Ambient Primary Biological Aerosol Particles (PBAP), Atmosphere, 9, 1–39, https://doi.org/10.3390/atmos9010001, 2017.

Fröhlich-Nowoisky, J., Kampf, C. J., Weber, B., Huffman, J. A., Pöhlker, C., Andreae, M. O., Lang-Yona, N., Burrows, S. M., Gunthe, S. S., Elbert, W., Su, H., Hoor, P., Thines, E., Hoffmann, T., Després, V. R., and Pöschl, U.: Bioaerosols in the Earth system: Climate, health, and ecosystem interactions, Atmos. Res., 182, 346–376, https://doi.org/10.1016/j.atmosres.2016.07.018, 2016.

Gabey, A. M.: Laboratory and field characterization of fluorescent and primary biological aerosol particles, Ph.D. thesis, University of Manchester, England, 2011.

Gabey, A. M., Gallagher, M. W., Whitehead, J., Dorsey, J. R., Kaye, P. H., and Stanley, W. R.: Measurements and comparison of primary biological aerosol above and below a tropical forest canopy using a dual channel fluorescence spectrometer, Atmos. Chem. Phys., 10, 4453–4466, https://doi.org/10.5194/acp-10-4453-2010, 2010.

Gabey, A. M., Vaitilingom, M., Freney, E., Boulon, J., Sellegri, K., Gallagher, M. W., Crawford, I. P., Robinson, N. H., Stanley, W. R., and Kaye, P. H.: Observations of fluorescent and biological aerosol at a high-altitude site in central France, Atmos. Chem. Phys., 13, 7415–7428, https://doi.org/10.5194/acp-13-7415-2013, 2013.

Gioda, A., Mayol-Bracero, O. L., Scatena, F. N., Weathers, K. C., Mateus, V. L., and McDowell, W. H.: Chemical constituents in clouds and rainwater in the Puerto Rican rainforest: Potential sources and seasonal drivers, Atmos. Environ., 68, 208–220, https://doi.org/10.1016/j.atmosenv.2012.11.017, 2013.

Gosselin, M. I., Rathnayake, C. M., Crawford, I., Pöhlker, C., Fröhlich-Nowoisky, J., Schmer, B., Després, V. R., Engling, G., Gallagher, M., Stone, E., Pöschl, U., and Huffman, J. A.: Fluorescent bioaerosol particle, molecular tracer, and fungal spore concentrations during dry and rainy periods in a semi-arid forest, Atmos. Chem. Phys., 16, 15165–15184, https://doi.org/10.5194/acp-16-15165-2016, 2016.

Healy, D. A., Huffman, J. A., O'Connor, D. J., Pöhlker, C., Pöschl, U., and Sodeau, J. R.: Ambient measurements of biological aerosol particles near Killarney, Ireland: a comparison between real-time fluorescence and microscopy techniques, Atmos. Chem. Phys., 14, 8055–8069, https://doi.org/10.5194/acp-14-8055-2014, 2014.

Hernandez, M., Perring, A. E., McCabe, K., Kok, G., Granger, G., and Baumgardner, D.: Chamber catalogues of optical and fluorescent signatures distinguish bioaerosol classes, Atmos. Meas. Tech., 9, 3283–3292, https://doi.org/10.5194/amt-9-3283-2016, 2016.

Ho, J., Spence, M., and Hairston, P.: Measurement of Biological Aerosol with a Fluorescent Aerodynamic Particle Sizer (FLAPS): Correlation of Optical Data with Biological Data, Aerobiologia, 15, 281–291, https://doi.org/10.1023/A:1007647522397, 1999.

Hoose, C., Kristjánsson, J. E., and Burrows, S. M.: How important is biological ice nucleation in clouds on a global scale?, Environ. Res. Lett., 5, 024009, https://doi.org/10.1088/1748-9326/5/2/024009, 2010.

Huffman, J. A. and Santarpia, J. L.: Online techniques for quantification and characterization of biological aerosol, in: Microbiology of Aerosols, edited by: Delort, A. M. and Amato, P., Wiley, Hoboken, NJ, chap. 1.4, John Wiley & Sons, Inc., New York, https://doi.org/10.1002/9781119132318.ch1d, 2017.

Jaenicke, R.: Abundance of cellular material and proteins in the atmosphere, Science, 308, p. 73, https://doi.org/10.1126/science.1106335, 2005.

Kaye, P. H., Stanley, W. R., Hirst, E., Foot, E. V., Baxter, K. L., and Barrington, S. J.: Single particle multichannel bio-aerosol fluorescence sensor, Opt. Express, 13, 3583–3593, 2005.

Kaye, P. H., Aptowicz, K., Chang, R. K., Foot, V., and Videen, G.: Angularly resolved elastic scattering from airborne particles – Potential for characterizing, classifying, and identifying individual aerosol particles, Opt. Biol. Part., 238, 31–61, 2007.

Kulkarni, P., Baron, P. A., and Willeke, K.: Aerosol Measurement: Principles, Techniques, and Applications, 3rd Edn., Wiley, ISBN 978-0-470-38741-2, 2011.

Möhler, O., DeMott, P. J., Vali, G., and Levin, Z.: Microbiology and atmospheric processes: the role of biological particles in cloud physics, Biogeosciences, 4, 1059–1071, https://doi.org/10.5194/bg-4-1059-2007, 2007.

Oliveira, M., Ribeiro, H., and Abreu, I.: Annual variation of fungal spores in atmosphere of Porto: 2003, Ann. Agric. Environ. Med., 12, 309–315, 2005.

Ortiz-Martínez, M. G., Rodríguez-Cotto, R. I., Ortiz-Rivera, M. A., Pluguez-Turull, C. W., and Jiménez-Vélez, B. D.: Linking Endotoxins, African Dust PM_{10} and Asthma in an Urban and Rural Environment of Puerto Rico, Mediators Inflamm., 2015, 784212, https://doi.org/10.1155/2015/784212, 2015.

Perring, A. E., Schwarz, J. P., Baumgardner, D., Hernandez, M. T., Spracklen, D. V., Heald, C. L., Gao, R. S., Kok, G., McMeeking, G. R., McQuaid, J. B., and Fahey, D. W.: Airborne observations of regional variation in fluorescent aerosol across the United States, J. Geophys. Res.-Atmos., 120, 1153–1170, https://doi.org/10.1002/2014JD022495, 2015.

Pope, F. D.: Pollen grains are efficient cloud condensation nuclei, Environ. Res. Lett., 5, 044015, https://doi.org/10.1088/17489326/5/4/044015, 2010.

Quintero, E., Rivera-Mariani, F., and Bolaños-Rosero, B.: Analysis of environmental factors and their effects on fungal spores in the atmosphere of a tropical urban area (San Juan, Puerto Rico), Aerobiologia, 26, 113–124, https://doi.org/10.1007/s10453-009-9148-0, 2010.

Raga, G. B., Baumgardner, D., and Mayol-Bracero, O. L.: History of aerosol-cloud interactions derived from observations in mountaintop clouds in Puerto Rico, Aerosol Air Qual. Res., 16, 674–688, https://doi.org/10.4209/aaqr.2015.05.0359, 2016.

Roberts, G. C. and Nenes, A.: A Continuous-Flow Streamwise Thermal-Gradient CCN Chamber for Atmospheric Measurements, Aerosol Sci. Technol., 39, 206–221, 2005.

Rivera-Mariani, F. E., Nazario-Jiménez, S., López-Malpica, F., and Bolaños-Rosero, B.: Sensitization to airborne ascospores, basidiospores, and fungal fragments in allergic rhinitis and asthmatic subjects in San Juan, Puerto Rico, Int. Arch. Allergy Immunol., 155, 322–334, https://doi.org/10.1159/000321610, 2011.

Rivera-Mariani, F. E., Almaguer, M., Aira, M. J., and Bolaños-Rosero, B.: Comparison of atmospheric fungal spore concentrations between two main cities in the Caribbean basin, P. R. Health Sci. J., 39, 235–242, 2020.

Sarangi, B., Baumgardner, D., Bolaños-Rosero, B., and Mayol-Bracero, O. L.: Dataset to: Measurement Report: An Exploratory Study of Fluorescence and CCN Activity of Urban Aerosols in San Juan, Puerto Rico, Mendeley Data [data set], Version 1, https://doi.org/10.17632/t26dctfk7t.1, 2021.

Savage, N. J., Krentz, C. E., Könemann, T., Han, T. T., Mainelis, G., Pöhlker, C., and Alex Huffman, J.: Systematic characterization and fluorescence threshold strategies for the wideband integrated bioaerosol sensor (WIBS) using size-resolved biological and interfering particles, Atmos. Meas. Tech., 10, 4279–4302, https://doi.org/10.5194/amt-10-4279-2017, 2017.

Spiegel, J. K., Buchmann, N., Mayol-Bracero, O. L., Cuadra-Rodriguez, L. A., Valle Díaz, C. J., Prather, K. A., Mertes, S., and Eugster, W.: Do Cloud Properties in a Puerto Rican Tropical Montane Cloud Forest Depend on Occurrence of Long-Range Transported African Dust?, Pure Appl. Geophys., 171, 2443–2459, https://doi.org/10.1007/s00024-014-0830-y, 2014.

Stanley, W. R., Kaye, P. H., Foot, V. E., Barrington, S. J., Gallagher, M., and Gabey, A.: Continuous bioaerosol monitoring in a tropical environment using a UV fluorescence particle spectrometer, Atmos. Sci. Lett., 12, 195–199, https://doi.org/10.1002/asl.310, 2011.

Stocker, T. F., Qin, D., Plattner, G.-K., Tignor, M., Allen, S. K., Boschung, J., Nauels, A., Xia, Y., Bex, V., and Midgley, P. M.: Climate change 2013: the physical science basis, Contribution of working group I to the fifth assessment report of the intergovernmental panel on climate change, IPCC, 2013, Cambridge University Press, Cambridge, United Kingdom and New York,

NY, USA, p. 1535, edited by: Stommel, E. W., Fiel, ISBN 978-1-107-05799-1, 2013.

Stolzenburg, M. R. and McMurry, P. H.: An Ultrafine Aerosol Condensation Nucleus Counter, Aerosol Sci. Tech., 14, 48–65, 1991.

Toprak, E. and Schnaiter, M.: Fluorescent biological aerosol particles measured with the Waveband Integrated Bioaerosol Sensor WIBS-4: laboratory tests combined with a one year field study, Atmos. Chem. Phys., 13, 225–243, https://doi.org/10.5194/acp-13-225-2013, 2013.

Torres-Delgado, E., Baumgardner, D., and Mayol-Bracero, O. L.: Measurement report: Impact of African aerosol particles on cloud evolution in a tropical montane cloud forest in the Caribbean, Atmos. Chem. Phys., 21, 18011–18027, https://doi.org/10.5194/acp-21-18011-2021, 2021.

Toro-Heredia, J., Jirau-Colón, H., and Jiménez-Vélez, B. D.: Linking $PM_{2.5}$ organic constituents, relative toxicity and health effects in Puerto Rico, Environ. Chall., 5, 100350, https://doi.org/10.1016/j.envc.2021.100350, 2021.

Twohy, C. H., McMeeking, G. R., DeMott, P. J., McCluskey, C. S., Hill, T. C. J., Burrows, S. M., Kulkarni, G. R., Tanarhte, M., Kafle, D. N., and Toohey, D. W.: Abundance of fluorescent biological aerosol particles at temperatures conducive to the formation of mixed-phase and cirrus clouds, Atmos. Chem. Phys., 16, 8205–8225, https://doi.org/10.5194/acp-16-8205-2016, 2016.

Valle-Díaz, C. J., Torres-Delgado, E., Colón-Santos, S. M., Lee, T., Collett, J. L., McDowell, W. H., and Mayol-Bracero, O. L.: Impact of long-range transported african dust on cloud water chemistry at a tropical montane cloud forest in Northeastern Puerto Rico, Aerosol Air Qual. Res., 16, 653–664, https://doi.org/10.4209/aaqr.2015.05.0320, 2016.

Velázquez-Lozada, A., González, J. E., and Winter, A.: Urban heat islands effect analysis for San Juan, Puerto Rico, Atmos. Environ., 40, 1731–1741, 2006.

Whitehead, J. D., Darbyshire, E., Brito, J., Barbosa, H. M. J., Crawford, I., Stern, R., Gallagher, M. W., Kaye, P. H., Allan, J. D., Coe, H., Artaxo, P., and McFiggans, G.: Biogenic cloud nuclei in the central Amazon during the transition from wet to dry season, Atmos. Chem. Phys., 16, 9727–9743, https://doi.org/10.5194/acp-16-9727-2016, 2016.

Uin, J.: Ultra-High Sensitivity Aerosol Spectrometer (UHSAS) instrument handbook, ARM Tech. Rep. DOE/SCARM-TR-163, USA, 17 pp., U.S. Department of Energy, doi.org/10.2172/1251410, 2016.

Zhang, M., Khaled, A., Amato, P., Delort, A.-M., and Ervens, B.: Sensitivities to biological aerosol particle properties and ageing processes: potential implications for aerosol–cloud interactions and optical properties, Atmos. Chem. Phys., 21, 3699–3724, https://doi.org/10.5194/acp-21-3699-2021, 2021.

Ziemba, L. D., Beyersdorf, A. J., Chen, G., Corr, C. A., Crumeyrolle, S. N., Diskin, G., Hudgins, C., Martin, R., Mikoviny, T., Moore, R., Shook, M., Lee Thornhill, K., Winstead, E. L., Wisthaler, A., and Anderson, B. E.: Airborne observations of bioaerosol over the Southeast United States using a Wideband Integrated Bioaerosol Sensor, J. Geophys. Res., 121, 8506–8524, https://doi.org/10.1002/2015JD024669, 2016.